

## Amplitude-phase control of a novel chaotic attractor

Chunbiao LI<sup>1,2,3,\*</sup>, İhsan PEHLİVAN<sup>2,4</sup>, Julien Clinton SPOTT<sup>2</sup>

<sup>1</sup>School of Electronic & Information Engineering, Nanjing University of Information Science & Technology, Nanjing, P.R. China

<sup>2</sup>Department of Physics, University of Wisconsin-Madison, Madison, WI, USA

<sup>3</sup>Engineering Technology Research and Development Center of Jiangsu Circulation Modernization Sensor Network, Jiangsu Institute of Commerce, Nanjing, P.R. China

<sup>4</sup>Department of Electrical and Electronics Engineering, Faculty of Technology, Sakarya University, Esentepe Campus, Serdivan, Sakarya, Turkey

Received: 09.01.2013

Accepted/Published Online: 14.05.2013

Final Version: 01.01.2016

**Abstract:** A novel chaotic attractor with a fractal wing structure is proposed and analyzed in terms of its basic dynamical properties. The most interesting feature of this system is that it has complex dynamical behavior, especially coexisting attractors for particular ranges of the parameters, including two coexisting periodic or strange attractors that can coexist with a third strange attractor. Amplitude and phase control methods are described since they are convenient for circuit design and chaotic signal applications. An appropriately chosen parameter in a particular quadratic coefficient can realize partial amplitude control. An added linear term can change the symmetry and provide an accessible knob to control the phase polarity. Finally, an amplitude-phase controllable circuit is designed using PSpice, and it shows good agreement with the theoretical analysis.

**Key words:** Fractal structure, amplitude control, phase control, coexisting attractors

### 1. Introduction

Chaotic systems and their dynamical behavior have inspired the interest of researchers because of their potential application in many fields, especially in the communication and information industries. Chaotic attractors are a signature of chaos and reveal its character. Recently, strange attractors with wing structures [1–11], such as the four-wing attractor [2–7] and multiwing attractor [8–11], have been of interest because of their elegant symmetry and multiple possible extensions. Furthermore, a chaotic flow generally has complexity and diversity. Some nonlinear dynamical systems exhibit hysteresis and coexisting attractors [12,13]. Wing structures not only consist of the main attractor branches, but also provide a bond between different parts of the phase trajectory. In this paper, we propose a novel chaotic attractor different from other ones [14–16], which exhibits four wing-like branches with a bond that has a double-wing structure. In this sense, the wing structure can penetrate the different regions of the attractor and the transition bonds. For selected parameters, two and even three coexisting attractors are observed.

On the other hand, adapting a chaotic system to engineering applications often requires synchronization [17–19] and amplitude-phase control [20,21]. However, the amplitude and the phase control parameters have not been discussed in chaotic systems with quadratic nonlinearity. In this paper, to achieve adequate amplitude

\*Correspondence: chunbiaolee@gmail.com

and phase control, we introduce a parameter in a quadratic coefficient to achieve partial amplitude control and to change the symmetry of the chaotic system to provide phase polarity control. A corresponding chaotic circuit is designed in PSpice, which confirms the theoretical analysis.

## 2. Novel chaotic attractor

Liu and Chen proposed a relatively simple three-dimensional continuous-time autonomous chaotic system [22] as follows.

$$\begin{cases} \dot{x} = ax - yz, \\ \dot{y} = -by + xz, \\ \dot{z} = -cz + xy, \end{cases} \quad (1)$$

This system possesses multiple symmetries in the equations and dynamical flow. Linear and nonlinear terms can be added to change the symmetry and behavior. We introduce a linear term  $-by$  in the third dimension of Eq. (1) to control the dynamics.

$$\begin{cases} \dot{x} = x - yz, \\ \dot{y} = -ay + xz, \\ \dot{z} = -by - cz + xy, \end{cases} \quad (2)$$

When  $a = 2.5$ ,  $b = 3.75$ , and  $c = 1.125$ , system (2) displays a novel chaotic attractor with a wing structure as shown in Figure 1 with initial conditions of  $(x_0, y_0, z_0) = (0, 1, -1)$ . The equations are solved with MATLAB using a fourth-order Runge–Kutta integrator with a fixed time step of 0.005. The added linear term is necessary to produce a real four-wing chaotic system. The calculated Lyapunov exponents are  $L_1 = 0.2712$ ,  $L_2 = 0$ , and  $L_3 = -2.8962$ , and the Kaplan–Yorke dimension is  $D_{KY} = 2 - L_1/L_3 = 2.0936$ .

Figure 2 shows cross-sections of the attractor in the planes  $x = 3$  and  $y = -3$ . These sections show six main branches, two of which consist of subbranches in what appears to be a fractal structure as expected for a strange attractor.

## 3. Basic dynamical properties

### 3.1. Equilibria

System (2) has five equilibria that can be found from the following.

$$\begin{cases} x - yz = 0, \\ -ay + xz = 0, \\ -by - cz + xy = 0, \end{cases} \quad (3)$$

For  $\alpha = \frac{b}{2}$ ,  $\beta = \frac{\sqrt{ab^2+4a^2c}}{2\sqrt{a}}$ ,  $\mu = \frac{b}{2\sqrt{a}}$ ,  $\omega = \frac{\sqrt{ab^2+4a^2c}}{2a}$ , the equilibria are  $P_1 = (0, 0, 0)$ ,  $P_2 = (\alpha + \beta, -\mu - \omega, -\sqrt{a})$ ,  $P_3 = (\alpha + \beta, \mu + \omega, \sqrt{a})$ ,  $P_4 = (\alpha - \beta, -\mu + \omega, -\sqrt{a})$ , and  $P_5 = (\alpha - \beta, \mu - \omega, \sqrt{a})$ . When  $a = 2.5$ ,  $b = 3.75$ , and  $c = 1.125$ , the corresponding equilibrium points are  $P_1 = (0, 0, 0)$ ,  $P_2 = (4.3906, -2.7768, -1.5811)$ ,  $P_3 = (4.3906, 2.7768, 1.5811)$ ,  $P_4 = (-0.6406, 0.4051, -1.5811)$ , and  $P_5 = (-0.6406, -0.4051, 1.5811)$ . Equilibrium points  $P_2$  and  $P_3$ , and  $P_4$  and  $P_5$  are symmetrical about the  $x$ -axis.

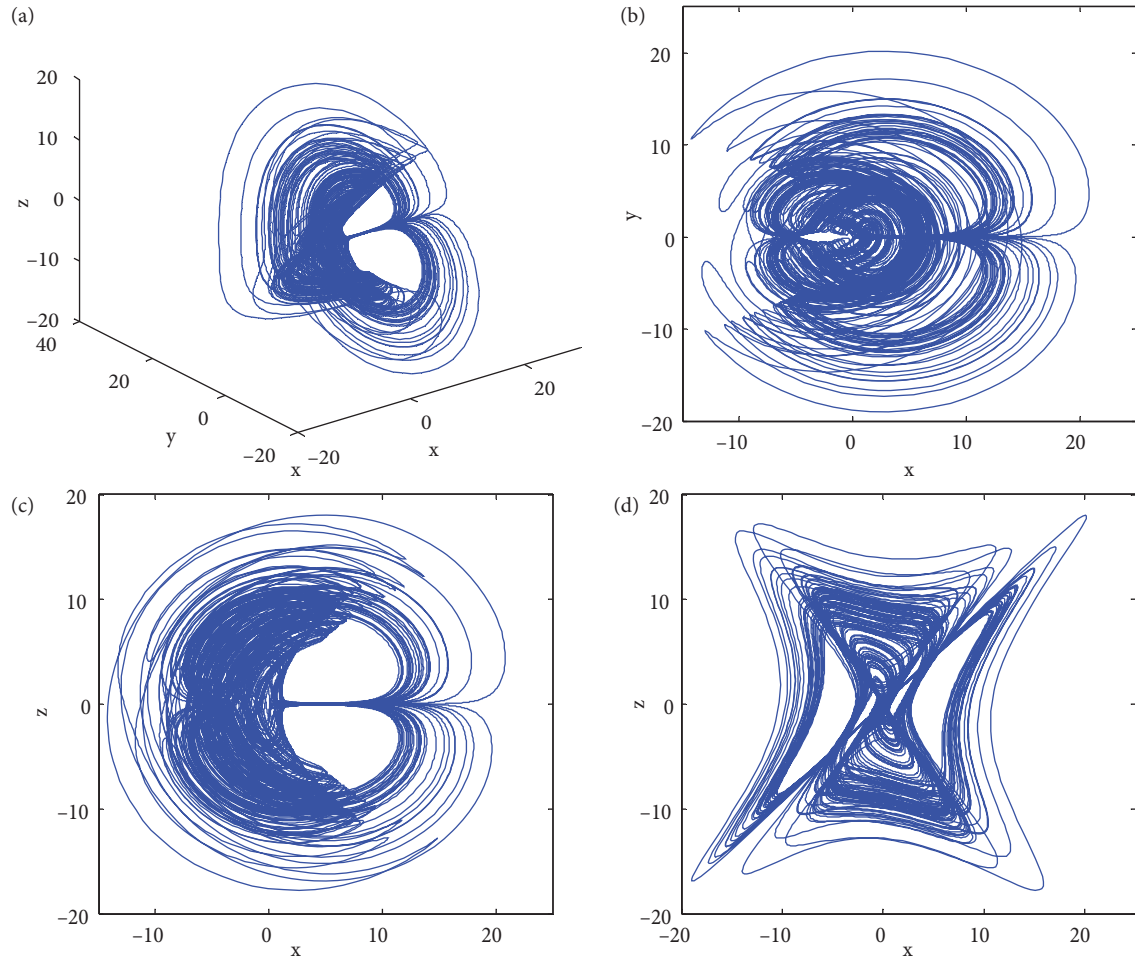


**Figure 1.** Chaotic attractor: (a) three-dimensional view, (b)  $x - y$  phase plane, (c)  $x - z$  phase plane, (d)  $y - z$  phase plane.

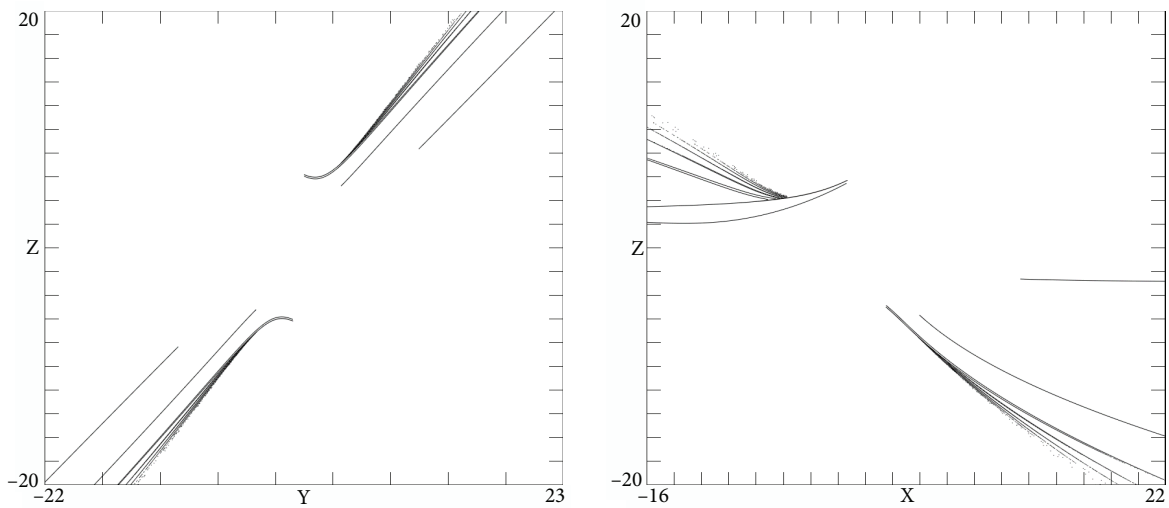


**Figure 2.** Cross-sections of the attractor in planes where (a)  $x = 3$ , (b)  $y = -3$ .

### 3.2. Jacobian matrices

The Jacobian matrix for system (2) at  $P_1 = (0, 0, 0)$  is:

$$J_1 = \begin{pmatrix} 1 & -z & -y \\ z & -a & x \\ y & -b+x & -c \end{pmatrix} = \begin{pmatrix} 1 & 0 & 0 \\ 0 & -2.5 & 0 \\ 0 & -3.75 & -1.125 \end{pmatrix}. \quad (4)$$

From  $|\lambda I - J_1| = 0$ , the eigenvalues of the Jacobian matrix  $J_1$  are  $\lambda_1 = 1$ ,  $\lambda_2 = -1.125$ , and  $\lambda_3 = -2.5$ . Since  $\lambda_1$  is a positive real number and the other two are negative real numbers, the equilibrium  $P_1$  is a saddle-node.

For the equilibrium  $P_2$ , the Jacobian matrix is:

$$J_2 = \begin{pmatrix} 1 & -z & -y \\ z & -a & x \\ y & -b+x & -c \end{pmatrix} = \begin{pmatrix} 1 & 1.5811 & 2.7768 \\ -1.5811 & -2.5 & 4.3906 \\ -2.7768 & 0.6406 & -1.125 \end{pmatrix}. \quad (5)$$

Here the eigenvalues are  $\lambda_1 = -3.8715$ ,  $\lambda_2 = 0.6232 + 3.3200i$ , and  $\lambda_3 = 0.6232 - 3.3200i$ .  $\lambda_1$  is a negative real number, and  $\lambda_2$  and  $\lambda_3$  are a pair of complex conjugate eigenvalues with positive real parts. Therefore, the equilibrium  $P_2$  is a saddle-focus. For the third equilibrium  $P_3$ , the eigenvalues of  $J_3$  are identical to  $J_2$ , and thus it is also a saddle-focus. For the equilibrium points  $P_4$  and  $P_5$ , the eigenvalues are identical and given by  $\lambda_1 = -3.4465$ ,  $\lambda_2 = 0.4107 + 1.3044i$ , and  $\lambda_3 = 0.4107 - 1.3044i$ , which is also a saddle-focus. Thus, system (2) is unstable at all equilibrium points.

### 3.3. Symmetry characteristics

System (1) has a unique rotational symmetry with respect to each of the axes as evidenced by its invariance under the coordinate transformations  $(x, y, z) \rightarrow (x, -y, -z)$ ,  $(x, y, z) \rightarrow (-x, y, -z)$ , and  $(x, y, z) \rightarrow (-x, -y, z)$ , respectively. An added linear term in any dimension can change the symmetry. The term  $-by$  in system (2) selects a specific symmetry with respect to the  $x$ -axis since the equations are then invariant only under the coordinate transformation  $(x, y, z) \rightarrow (x, -y, -z)$ . All equilibrium points are also symmetric with respect to the  $x$ -axis. Thus, the added term changes the symmetry and provides an accessible knob to control the phase polarity.

## 4. Amplitude-phase control and coexisting attractors

### 4.1. Amplitude control

Although it is possible to linearly rescale all the variables to avoid exceeding amplitude limitations of the hardware, it turns out that partial amplitude control is achieved by adding a coefficient  $d$  in the quadratic term  $-yz$  in the first dimension of system (2).

$$\begin{cases} \dot{x} = x - dyz, \\ \dot{y} = -ay + xz, \\ \dot{z} = -by - cz + xy, \end{cases} \quad (6)$$

If we take  $d \rightarrow kd$ ,  $x \rightarrow x$ ,  $y \rightarrow y/\sqrt{k}$ ,  $z \rightarrow z/\sqrt{k}$  ( $k > 0$ ) in Eq. (6), the resulting system is identical to system (2), which means that parameter  $d$  can control the amplitude of variables  $y$  and  $z$  according to  $1/\sqrt{k}$  while leaving the variable  $x$  unchanged.

The expected behavior is verified by numerical calculations as shown in Figure 3, which also shows that to within numerical error, the Lyapunov exponent spectrum is independent of  $d$ , as desired. This works because the first equation of system (6) has a single nonlinear term, and the second two equations are first-order in  $y$  and  $z$ , suggesting a general principle. Conversely,  $d$  would be a bad parameter to choose for studying bifurcations.

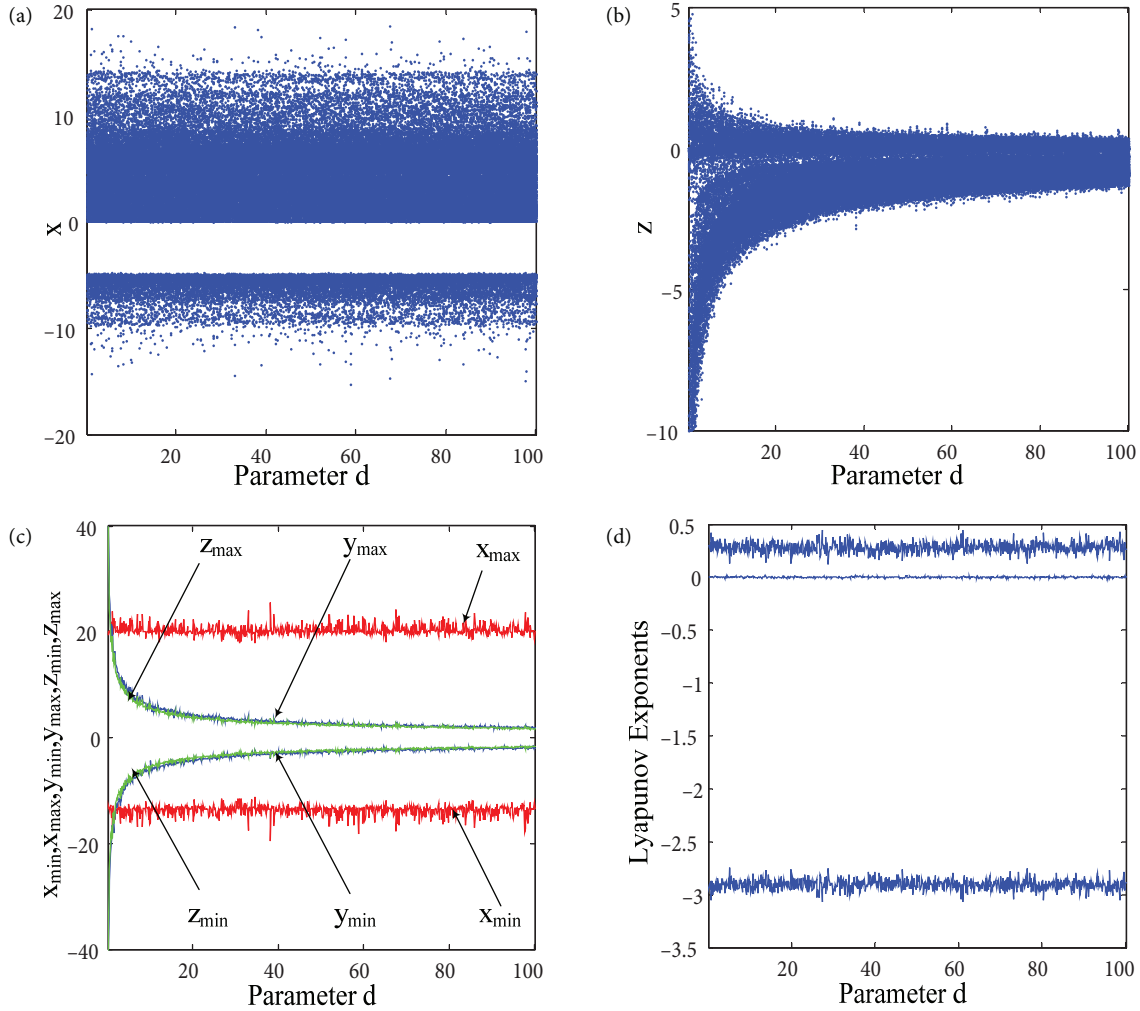


**Figure 3.** Amplitude parameter  $d$  adjusted the range of  $y$  and  $z$  without altering  $x$ : (a)  $x - d$  bifurcation diagram at  $y = 0$ , (b)  $z - d$  bifurcation diagram at  $y = 0$ , (c) range of variables, (d) Lyapunov exponents.

#### 4.2. Phase control and coexisting attractors

System (2) has three quadratic terms and four linear terms. Amplitude control parameters generally involve the coefficient of a nonlinear term, while phase control involves the coefficient of a linear term. In system (2), phase polarity can be controlled by changing the sign of  $b$ . The system is invariant to the transformation  $b \rightarrow -b$ ,  $x \rightarrow -x$ ,  $y \rightarrow -y$ ,  $z \rightarrow z$ , and thus  $b$  controls the phase of  $x$  and  $y$  as shown in Figure 4.

The bifurcation diagrams for  $x$  and  $y$  are reverse symmetrical, and the Lyapunov exponent spectrum is symmetrical in the negative and positive regions, confirming that changing the sign of  $b$  reverses the polarity of  $x$  and  $y$ , independent of whether the dynamics are chaotic. In particular, when  $b$  is chosen at  $-3.75$  and

3.75 with initial values  $(0, -1, -1)$  and  $(0, 1, -1)$ , respectively, the phases of the chaotic signals  $x(t)$  or  $y(t)$  are reversed as shown in Figure 5 despite the sensitive dependence on initial conditions. Generally, when phase polarity is reversed, the signs of the corresponding initial conditions also need to be changed to remain within the basin of attraction.

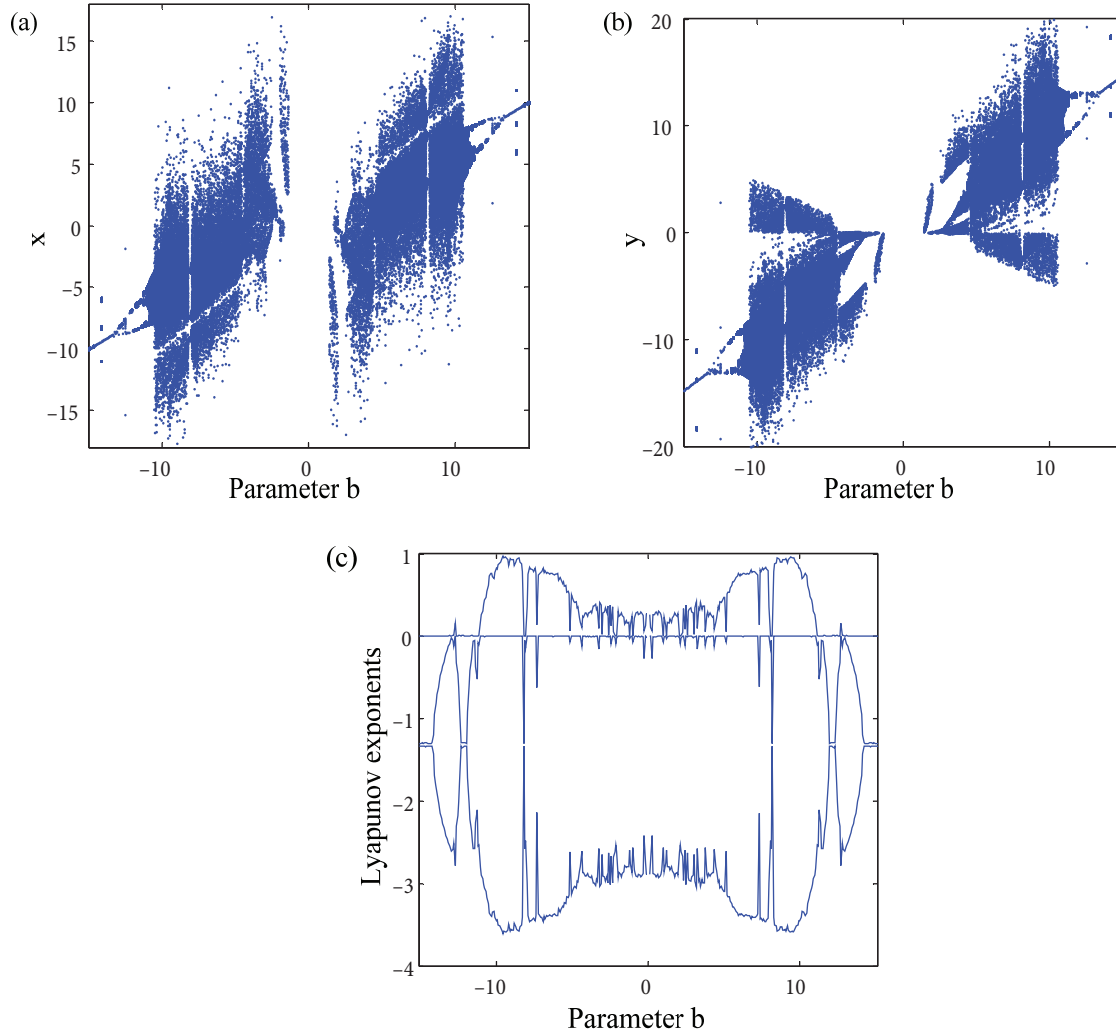


**Figure 4.** Bifurcation dynamics at  $z = 0$  when  $b$  varies in  $[-15, 15]$ : (a)  $x-b$  bifurcation diagram, (b)  $y-b$  bifurcation diagram, (c) Lyapunov exponents (with initial values  $(0, -1, -1)$  and  $(0, 1, -1)$  in the negative and positive regions, respectively).

Furthermore, system (2) has complex dynamical behavior in the region  $[-15, 15]$ , including the existence of coexisting attractors. Some chaotic attractors are shown in Figure 6 for various values of  $b$ . For  $b = 0.5$  and an initial condition of  $(0, 1, \pm 5)$ , system (2) has two two-wing attractors as shown in Figure 6a, where the dashed line is for the initial condition  $(0, 1, 5)$ . Moreover, when  $b = 1.37$ , system (2) has two attractors, which are periodic at  $b = 1.36$ . With an increase in  $b$ , the two two-wing structures coalesce and become a single four-wing attractor as shown in Figures 6b and 6c. For  $b$  greater than about 6, system (2) has three attractors, two of which are symmetric in  $z$ . For  $b = 7.8$ , the chaotic attractor coexists with two stable limit cycles as shown in Figure 6d, where the limit cycles are shown with a dashed line for the initial conditions  $(7, \pm 13, \pm 23)$ . When

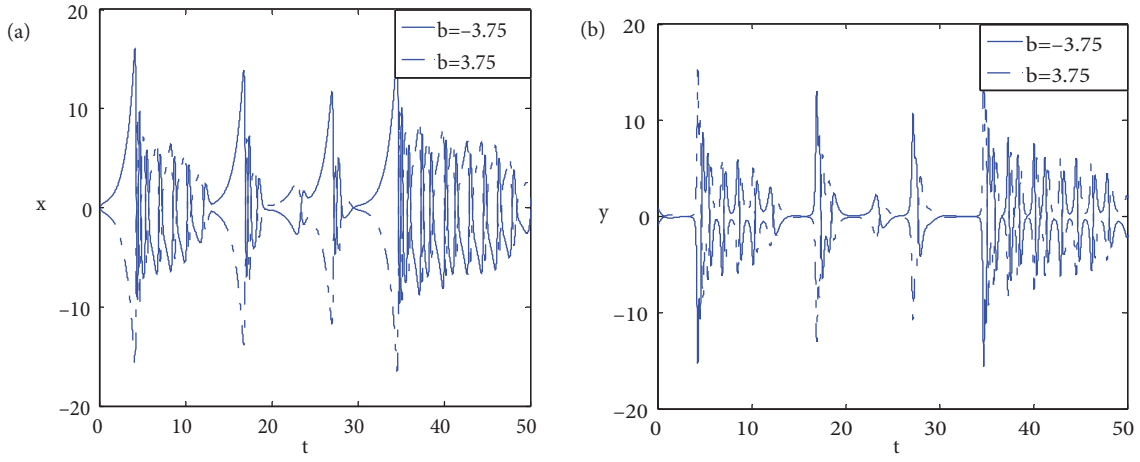


**Figure 5.** Phase polarity control: (a)  $x$  versus  $t$ , (b)  $y$  versus  $t$ .

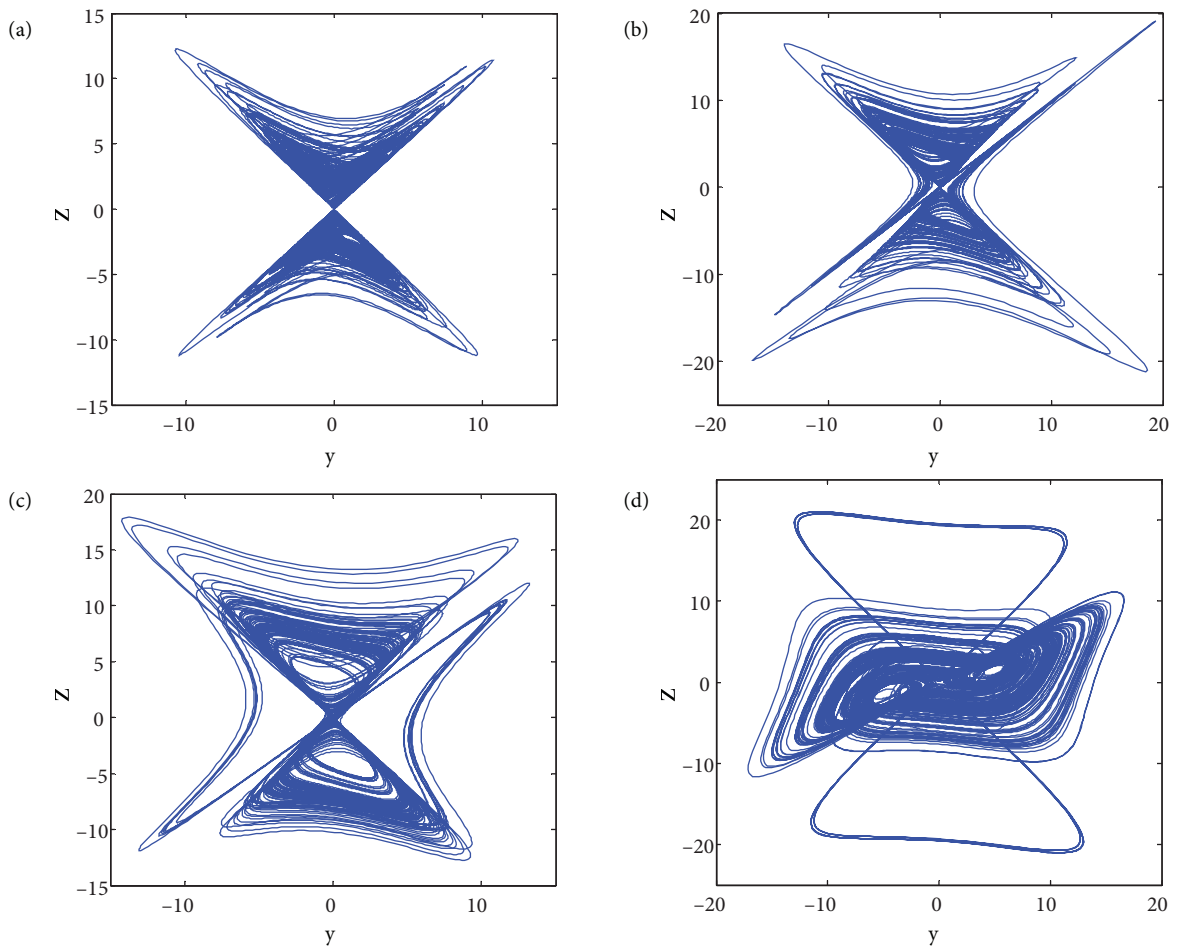


**Figure 6.** Phase portrait in the  $y - z$  plane with initial values  $(0, 1, -5)$  for (a)  $b = 0.5$ , (b)  $b = 1.6$ , (c)  $b = 2.8$ , and (d)  $b = 7.8$ .

$b = 9.5$ , system (2) has its maximum largest Lyapunov exponent of  $L_1 = 0.9608$  and Kaplan–Yorke dimension of  $D_{KY} = 2.276$ .

## 5. Chaotic circuit design

Amplitude control is important for circuit design and engineering applications because of hardware limitations. To avoid saturating analog multipliers and operational amplifiers, the circuit signal amplitude is usually reduced by a linear rescaling of the variables. However, many chaotic systems with symmetry, like system (2), include a knob to achieve partial amplitude control. In such a case, total amplitude control requires additional control only for the remaining uncontrolled variable(s).

In Figure 1, we see that all of the signals,  $x$ ,  $y$ , and  $z$ , oscillate in the interval of  $(-20, 20)$ . Considering the amplitude control of  $y$  and  $z$  by the parameter  $d$ , only the variable  $x$  needs to be rescaled. Letting  $u = x/2$ ,  $v = y$ , and  $w = z$ , and then setting the original state variables  $x$ ,  $y$ ,  $z$  instead of the variables  $u, v, w$ , the rescaled phase-controllable system becomes the following.

$$\begin{cases} \dot{x} = x - \frac{d}{2}yz, \\ \dot{y} = -ay + 2xz, \\ \dot{z} = \pm by - cz + 2xy, \end{cases} \quad (7)$$

From Eq. (7), we design the amplitude-phase adjustable analog circuit shown in Figure 7. The circuit equations in terms of the circuit parameters are:

$$\begin{cases} \dot{x} = \frac{1}{R_1 C_1} x - \frac{1}{R_2 C_1} yz, \\ \dot{y} = -\frac{1}{R_3 C_2} y + \frac{1}{R_4 C_2} xz, \\ \dot{z} = \pm \frac{1}{R_5 C_3} y - \frac{1}{R_6 C_3} z + \frac{1}{R_7 C_3} xy, \end{cases} \quad (8)$$

The circuit consists of three channels to realize the integration, addition, and subtraction of the state variables  $x$ ,  $y$ , and  $z$ , respectively. The operational amplifier OPA404/BB and its peripheral circuit perform the addition, inversion, and integration, and the analog multiplier AD633/AD performs the nonlinear product operation. The state variables  $x, y$ , and  $z$  in Eq. (8) correspond to the state voltages of the three channels, respectively. For the system parameters  $a = 2.5$ ,  $b = 3.75$ ,  $c = 1.125$ , and  $d = 4$ , the circuit element values are  $R_1 = 40 \text{ k}\Omega$ ,  $R_2 = R_4 = R_7 = 2 \text{ k}\Omega$ ,  $R_3 = 16 \text{ k}\Omega$ ,  $R_5 = 10.66 \text{ k}\Omega$ ,  $R_6 = 35.55 \text{ k}\Omega$ ,  $R_7 = 2 \text{ k}\Omega$ , and  $R_8 = R_9 = R_{10} = R_{11} = 10 \text{ k}\Omega$ . We select the capacitor  $C_1 = C_2 = C_3 = 10 \text{ nF}$  to obtain a stable phase portrait, which only affects the time scale of the oscillation. Figure 8 shows the phase portraits predicted by PSpice circuit simulation.

Unlike other chaotic circuits, here a potentiometer  $R_2$  is required to realize amplitude control. Generally, we first put the resistance at an extreme value and then adjust the control knob so that the voltages satisfy the requirements of the hardware. With a decrease in  $R_2$ , the amplitude of  $y$  and  $z$  decrease accordingly.

Furthermore, phase polarity control is implemented in the circuit. A polarity change of  $b$  is realized by the switch that provides the appropriate feedback of the signal  $y$ . The corresponding phase trajectories predicted by PSpice simulation are shown in Figure 9.



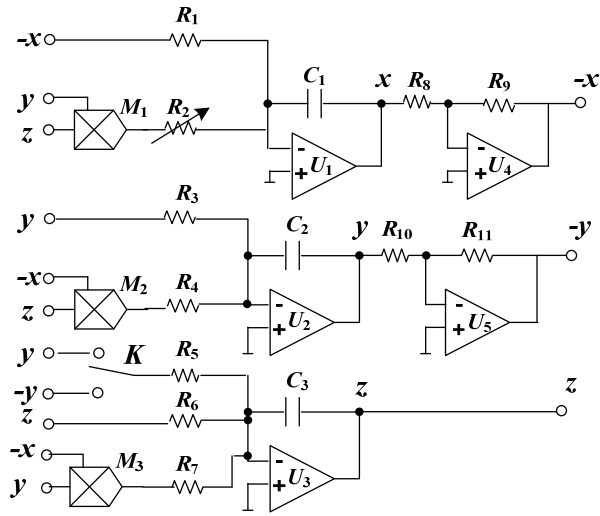


Figure 7. Amplitude-phase adjustable chaotic circuit.

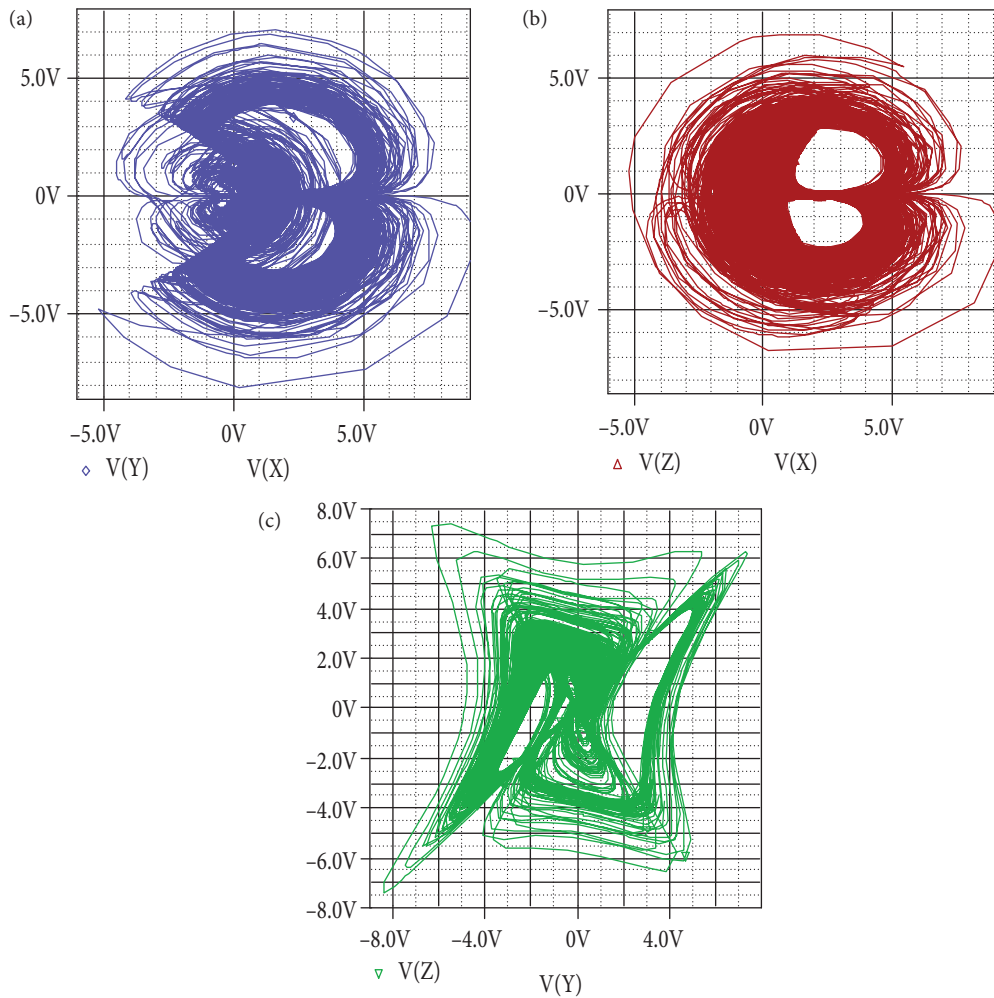
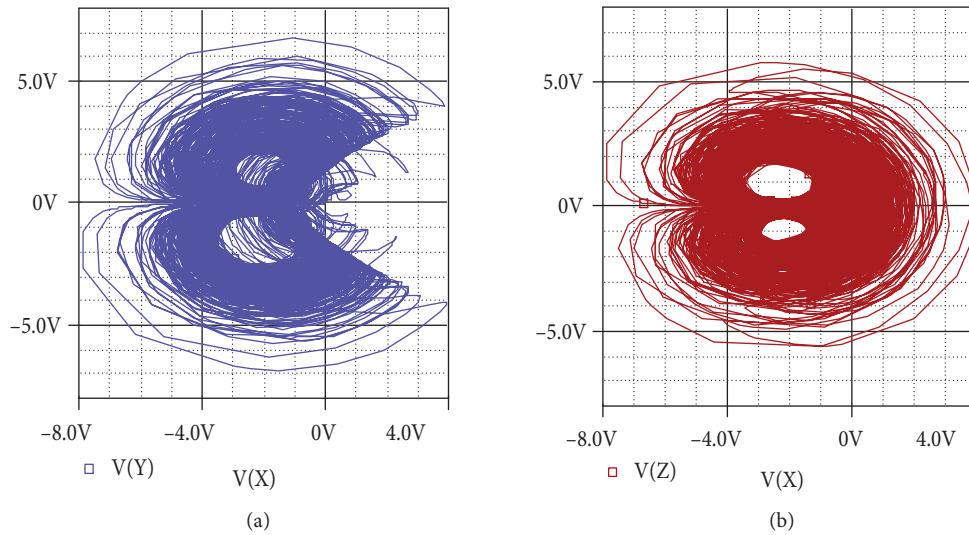


Figure 8. Phase portraits of system (2) in PSpice simulation with initial values  $x(0) = 0$ ,  $y(0) = -1$ , and  $z(0) = -1$ : (a) attractor in the  $x - y$  plane (1 V/div), (b)  $x - z$  plane (1 V/div), and (c)  $y - z$  plane (1 V/div).



**Figure 9.** Phase polarity of  $x$  and  $y$  reversed: (a) phase portrait in the  $x - y$  plane (1 V/div) and (b)  $x - z$  plane (1 V/div).

## 6. Conclusion

An added linear term in a pseudo four-wing system extracts the main four-wing structure with a special wing bond and produces a novel chaotic attractor. Its dynamical behavior is analyzed, especially coexisting attractors and amplitude and phase control. Due to the symmetry and system structure, a control method for amplitude and phase is established by introducing a parameter in the coefficient of a specific nonlinear term to achieve partial amplitude control, and a parameter is added in a linear term to alter the symmetry and allow phase polarity control. The corresponding amplitude-phase adjustable circuit is designed. The amplitude of two signals can be smoothly controlled, and the size of the corresponding attractors can be adjusted by a potentiometer. Furthermore, the phase polarity can be controlled by a simple switch. The results of PSpice circuit simulation show good agreement with the theoretical analysis. These special properties of the system provide a convenient passage to realize amplitude adjusting and phase adjusting in electronic engineering, especially in communication systems and radar systems. Even though the modified version seems more complicated and costly, the simple knobs to realize amplitude and phase control actually save some extra circuits to construct a much more complicated system.

## Acknowledgments

The research described in this publication was supported by the China Postdoctoral Science Foundation (Grant No. 2011M500838, 2012T50456) and the Postdoctoral Science Foundation of Jiangsu Province (Grant No. 1002004C), and also in part by the Jiangsu Overseas Research Training Program for University Prominent Young and Middle-Aged Teachers and Presidents, the 4th 333 High-Level Personnel Training Project (Su Talent [2011] No. 15) of Jiangsu Province.

## References

- [1] Özoğuz S, Elwakil AS, Kennedy MP. Experimental verification of the butterfly attractor in a modified Lorenz system. *Int J Bifur Chaos* 2002; 12: 1627–1632.

- [2] Liu X. A new 3D four-wing chaotic system with cubic nonlinearity and its circuit implementation. *Chin Phys Lett* 2009; 26: 090504.
- [3] Dong E, Chen Z, Chen Z, Yuan Z. A novel four-wing chaotic attractor generated from a three-dimensional quadratic autonomous system. *Chin Phys B* 2009; 18: 2680–2689.
- [4] Qi G, Chen G, Li S, Zhang Y. Four-wing attractors: from pseudo to real. *Int J Bifur Chaos* 2006; 16: 859–885.
- [5] Cang S, Qi G. A four-wing-hyper-chaotic attractor and transient chaos generated from a new 4-D quadratic autonomous system. *Nonlinear Dynam* 2010; 46: 263–270.
- [6] Elwakil AS, Özoğuz S, Kennedy MP. A four-wing butterfly attractor from a fully-autonomous system. *Int J Bifur Chaos* 2003; 13: 3093–3098.
- [7] Elwakil AS, Özoğuz S, Kennedy MP. Creation of a complex butterfly attractor using a novel Lorenz-type system. *IEEE T Circuits-I* 2002; 49: 527–530.
- [8] Yu S, Lu J, Chen G, Yu X. Design and implementation of grid multiwing butterfly chaotic attractors from a piecewise Lorenz system. *IEEE T Circuits-II* 2010; 57: 803–807.
- [9] Yu S, Lu J, Yu X, Chen G. Design and implementation of grid multi-wing hyperchaotic Lorenz system family via switching control and constructing super-heteroclinic loops. *IEEE T Circuits-I* 2012; 59: 1015–1028.
- [10] Yu S, Lu J, Chen G, Yu X. Generating grid multiwing chaotic attractors by constructing heteroclinic loops into switching systems. *IEEE T Circuits-II* 2011; 58: 314–318.
- [11] Elwakil AS, Özoğuz S. A system and a circuit for generating multi-butterflies. *Int J Bifur Chaos* 2008; 18: 841–845.
- [12] Sprott C, Wang X, Chen G. Coexistence of point, periodic and strange attractors. *Int J Bifur Chaos* 2013; 23: 1350093.
- [13] Qu S, Lu Y, Zhang L, He D. Discontinuous bifurcation and coexistence of attractors in a piecewise linear map with a gap. *Chinese Phys B* 2008; 17: 4418.
- [14] Pehlivan İ, Uyaroğlu Y. Simplified chaotic diffusionless Lorenz attractor and its application to secure communication systems. *IET Commun* 2007; 1: 1015–1022.
- [15] Pehlivan İ, Uyaroğlu Y. A new chaotic attractor from general Lorenz system family and its electronic experimental implementation. *Turk J Electr Eng Co* 2010; 18: 171–184.
- [16] Sundarapandian V, Pehlivan I. Analysis, control, synchronization and circuit design of a novel chaotic system. *Math Comput Model* 2012; 55: 1904–1915.
- [17] Boccaletti S, Kurths J, Osipov G, Valladares DL, Zhou C. The synchronization of chaotic systems. *Phys Rep* 2002; 366: 1–101.
- [18] Lu J, Yu X, Chen G. Chaos synchronization of general complex dynamical networks. *Physica A* 2004; 334: 281–302.
- [19] Li C, Chen S, Zhu H. Circuit implementation and synchronization of an improved system with invariable Lyapunov exponent spectrum. *Acta Phys Sin* 2009; 58: 2255–2265.
- [20] Li C, Wang H. An extension system with constant Lyapunov exponent spectrum and its evolvement study. *Acta Phys Sin* 2009; 58: 7514–7524.
- [21] Li C, Wang J, Hu W. Absolute term introduced to rebuild the chaotic attractor with constant Lyapunov exponent spectrum. *Nonlinear Dynam* 2012; 68: 575–587.
- [22] Liu W, Chen G. A new chaotic system and its generation. *Int J Bifur Chaos* 2003; 13: 261–267.